PASJ: Publ. Astron. Soc. Japan **52**, –?? (2008)

Near-Infrared Spectroscopy of the Cool Brown Dwarf, SDSS 1624+00

Tadashi Nakajima
National Astronomical Observatory, 2-21-1 Osawa, Mitaka, 181-8588
E-mail(TN): tadashi.nakajima@nao.ac.jp

Takashi Tsuji
Institute of Astronomy, University of Tokyo, 2-21-1 Osawa, Mitaka, 181-8588

Toshinori Maihara, Fumihide Iwamuro, Ken-taro Motohara, Tomoyuki Taguchi, Ryuji Hata
Department of Physics, Kyoto University, Kitashirakawa, Kyoto 606-8502

Motohide Tamura
National Astronomical Observatory, 2-21-1 Osawa, Mitaka, 181-8588
and
Takuya Yamashita
Subaru Telescope, National Astronomical Observatory of Japan, 650 North A′ohoku Place Hilo, Hawaii 96720, USA

(Received ; accepted)

Abstract

Using the Subaru Telescope, we have obtained multiple near-infrared spectra of the cool brown dwarf, SDSS 1624+00 (J162414.37+002915.8), in search of spectral variability in an 80 minute time span. We have found the suspected variability of water vapor absorption throughout the observations, which requires confirmation with a longer time baseline. After coadding the spectra, we have obtained a high-quality spectrum covering from 1.05 to 1.8 μm. There are three kinds of spectral indicators, the water vapor bands, methane band and K I lines at 1.243 and 1.252 μm, which can be used to study temperature and the presence of dust. We compare the spectra of SDSS 1624+00 and Gliese 229B, paying special attention to these indicators. The shallower water vapor absorption of SDSS 1624+00 indicates that it is warmer and/or dustier. The shallower methane absorption suggests that SDSS 1624+00 is warmer. We interpret the deeper K I lines in SDSS 1624+00 as the result of its higher temperature. With the help of model spectra, we conclude that SDSS 1624+00 is warmer and dustier than Gliese 229B. For the first time in a cool brown dwarf, a finite flux is seen at the bottom of the water vapor band between 1.34 and 1.42 μm, which means that the 1.4 μm band of water can completely be observed from the ground.

Key words: Spectroscopy — Stars: low-mass

1. Introduction

Until recently, Gliese 229B (hereafter Gl 229B) (Nakajima et al. 1995) had been the only brown dwarf cool enough to show methane absorption in its spectrum (Oppenheimer et al. 1995). It is still the only cool brown dwarf companion to a nearby star. In 1999, two large scale sky surveys, the Sloan Digital Sky Survey (Strauss et al. 1999) and the 2MASS (Burgasser et al. 1999) discovered six methane brown dwarfs in the field. Detailed studies of methane brown dwarfs, or T dwarfs (Kirkpatrick et al. 1999), are now becoming possible. Cuby et al. (1999) have found a very faint methane brown dwarf, despite observational difficulty.

The only T dwarf whose optical and infrared spectra have been studied in detail is Gl 229B (Geballe et al. 1996, Oppenheimer et al. 1998). Optical and infrared spectra have been obtained of SDSS 1624+00 (Strauss et al. 1999) and low-resolution infrared spectra have been obtained of the four 2MASS T dwarfs (Burgasser et al. 1999). The spectrum of Gl 229B is characterized by broad methane and water vapor absorption bands (Oppenheimer 1995). The details of methane and water vapor features were studied by Geballe et al. (1996).

Two groups have reported the detection of CO in Gl 229B (Noll et al. 1997, Oppenheimer et al. 1998). The presence of CO is not consistent with the cool environment of the T dwarf, and some mechanism that brings up CO to upper atmosphere from a deep hot region must exist. As for atomic lines, Oppenheimer et al. (1998) identified two Cs I lines in the far optical spectrum of Gl 229B. One of the Cs I lines is also seen the spectrum of SDSS 1624+00 by Strauss et al. (1999) who have found that two K I lines in the J band are stronger in SDSS

1624+00 than Gl 229B.

Weather has been searched for in a couple of warm brown dwarfs by spectral variability (Tinney and Tolley 1999). A large number of warm brown dwarfs are seen to be rapidly rotating (Martín et al. 1997, Tinney and Reid 1998), and rotation periods expected from rotation velocities are 3−6 h, comparable to the rotation period of the Jupiter. So it seems reasonable to assume that the rotation periods of cool brown dwarfs are of the same order. Tinney and Tolley did not find any variability of the L-type brown dwarf DENIS-PJ1228-1547, but found the variability of the M-type brown dwarf LP 944-20.

In this paper, we report the results of a search for spectral variability of SDSS 1624+00 in the near infrared. An integrated spectrum with high signal-to-noise ratio is used for detailed investigation of spectral features in comparison with the previously obtained Gl 229B spectra by Geballe et al. (1996) and Oppenheimer et al (1998).

2. Observations and Data Reduction

Observations were carried out on 1999 June 20 (UT) on the Subaru Telescope, using the grism mode of the Cooled Infrared Spectrograph and Camera for OH Suppression Spectrograph (CISCO) which employs a 1024×1024 HgCdTe array. The slit width of $0\farcs7$ corresponds to a resolution of 0.005 μm in the wavelength range from 1.05 to 1.8 μm. The pixel scale of $0\farcs116$/pix gives six pixels per resolution. The sky was almost clear, but the image size varied between 0.4 and $1''$. We obtained 27 useful 100 second exposures between 10:53 and 12:13 UT, which were once interrupted by a telescope tracking error. The log of observing is given in table 1.

Within the slit length of $119''$, a nearby bright star $56\farcs7$ away was observed simultaneously to the target brown dwarf. For sky cancellation, both the object and the nearby star were shifted along the slit. This nearby star was used to monitor the possible variation of transmission. Apart from the nearby star, the A0 star SAO121542 (V = 7.7) and the F2 star SAO121611 (V = 9.0), were observed for reference after the target observations.

IRAF was used for data reduction. Each frame was sky subtracted and then divided by the average dome flat frame. The flattened frame was distortion corrected and wavelength calibrated, using OH airglow lines. Then the spectra of SDSS 1624+00 and the nearby star were extracted.

The spectral type of the nearby bright star is unknown. By the comparison of the continuum slopes of the nearby star, A0 star, and F2 star, the effective temperature of the nearby star was estimated to be 4800K. This estimate is consistent with the presence of weak Paβ absorption in the nearby star spectrum.

Table 1. Log of observations.

Spectrum	Start time (1999 June 20 UT)	Comment
1	10:53:03	
2	10:54:47	
3	10:56:32	
4	10:58:17	
5	11:32:53	Interruption before observing
6	11:34:37	
7	11:36:22	
8	11:38:07	
9	11:39:52	
10	11:42:18	
11	11:44:03	
12	11:45:48	
13	11:47:32	
14	11:49:17	
15	11:51:02	
16	11:53:22	
17	11:55:07	
18	11:56:52	
19	11:58:37	
20	12:00:22	
21	12:02:07	
22	12:04:27	
23	12:06:12	
24	12:07:58	
25	12:09:43	
26	12:11:28	
27	12:13:12	

Table 2. Combined spectra.

Combined spectrum	Original Spectra
A	1, 2, 3, 4
B	5, 6, 7, 8, 9
C	8, 9, 10, 11, 12
D	11, 12, 13, 14, 15
E	14, 15, 16, 17, 18
F	17, 18, 19, 20, 21
G	20, 21, 22, 23, 24
H	23, 24, 25, 26, 27
I	1 – 27

No photometry for absolute flux calibration was obtained. The relative flux of each object spectrum was calibrated by dividing by the nearby star spectrum in the same frame and multiplying by a 4800K blackbody spectrum. In figure 1, the ratio of the first nearby star spectrum to the last is plotted. From the figure, it is apparent that transmission variation due to telluric water vapor was significant over the time scale of 80 minutes, and that the calibration by the simultaneously observed nearby star was essential.

3. Discussion

3.1. Variability

In order to discuss variability, one must know the level of noise in each spectrum obtained in 100 seconds. The major source of noise is shot noise in OH airglow lines. To see the influence of the OH lines, a sky spectrum was extracted using the same aperture for object and its square root was calculated. The square root of the sky spectrum is shown in figure 2 along with a typical raw spectrum of SDSS 1624+00 which is not calibrated for wavelength and flux.

We have inspected calibrated spectra for 100 second exposures and found some possible variations, but they are not definitive in view of the limited signal-to-noise ratio. To see longer term variability and to improve the signal-to-noise ratio, four or five spectra were coadded to produce one spectrum corresponding to several minutes of observing. The combination of the spectra is shown in table 2.

Time series of the spectra denoted by A through H and the integrated spectrum denoted by I are shown in figure 3. The observations of A were more than 30 minutes before B due to interruption by the telescope tracking problem. Two types of small variation are seen in the time series. One is seen between A and the rest of the spectra, and the other is found throughout the time span. The major difference between A and the rest is the absorption features at 1.066 and 1.081 μm. These features are seen in three of the four original 100 second spectra. The left shoulder of the H band pseudo-continuum appears to vary continuously. The sawtooth pattern which extends from 1.53 to 1.58 μm in the spectra E and F is not clear in A and H. The pattern gradually grows to the left from A to F and becomes less obvious from F to H. To emphasize this variation, the average spectrum of A and H and that of E and F are compared in figure 4 in which vertical dotted lines indicate the locations of the three valleys of the sawteeth. It is likely that at least the latter type of variation is due to water vapor. To confirm the presence of this variability, we plan observations with a longer time baseline. The possible variation at 1.668 μm coincides with the location of a strong OH line and its reality is doubtful.

3.2. Integrated Spectrum

Here we discuss the details of the integrated spectrum in comparison with the previously obtained spectra of Gl 229B by Geballe et al. (Geballe et al. 1996, Leggett et al. 1999) and Oppenheimer et al. (1998) and with the spectrum of SDSS 1624+00 by Strauss et al. (1999). Geballe et al. and Strauss et al. obtained their spectra with CGS4 on UKIRT and Oppenheimer et al. with NIRC on Keck.

One major difference between Gl 229B and SDSS 1624+00 is that the former is brighter by 1.2 mag. Strauss et al. emphasize the similarity in the spectra of the two methane brown dwarfs and assume the same effective temperature and luminosity to drive the distance to SDSS 1624+00. However we have found from an analysis of model spectra described later that the overall near-infrared spectrum does not change significantly in the temperature range between 900K and 1100K apart from the absolute flux level which is unknown for SDSS 1624+00. So individual spectral features which are sensitive to temperature and dust need to be utilized.

Our integrated spectrum I of SDSS 1624+00 and the Gl 229B spectrum by Geballe et al. are plotted in figure 5 in log f_ν. Strauss et al. find that the significant difference is the excess of flux around 1.7 μm in SDSS 1624+00 and the stronger lines of K I 1.2432 and 1.2522 μm. Our findings are basically the same, the deeper methane feature including the region around 1.7 μm in Gl 229B and the stronger K I lines in SDSS 1624+00. In addition from the Gl 229B spectrum of Oppenheimer et al., we find that the water vapor absorption bands at 1.15 μm and 1.4 μm are deeper in Gl 229B. The signal-to-noise ratio of the water vapor absorption bands of the Gl 229B spectrum of Geballe et al. is limited, but that of Oppenheimer et al. is valid to the edges of bottoms of the absorption bands. From the analysis of the model spectra, we have found that these features are sensitive to temperature and the presence of dust.

In figure 6, six model spectra are plotted for dusty and dust free models for temperatures, 900, 1000K and 1100K. Here, the dust free model describes the situation that dust has formed, but has been segregated from the gas throughout the photosphere, and hence plays little role as a source of opacity. On the other hand, in the dusty model, dust is active as a source of opacity in the warm region deep in the photosphere (Tsuji et al. 1999). The models show following tendencies for the above mentioned spectral features. The methane absorption is deeper at the lower temperature and the K I lines are stronger at the higher temperature. Therefore the methane absorption indicates that Gl 229B is cooler, and the K I lines suggest that SDSS 1624+00 is warmer. From above information alone, one may judge that SDSS 1624+00 is warmer and the atmosphere is dust free. However, the situation is more complicated. We have detected a finite flux at the bottom of water vapor absorption between 1.34 and 1.42 μm in SDSS 1624+00, and the water vapor absorption is deeper in Gl 229B. According to the models, the water vapor absorption is deeper at the lower temperature and shallower in the dustier object. The dust free model tends to produce excessively deep water vapor absorption in SDSS 1624+00 and the shallowness of the trough is more consistent with the dusty model. From the spectral features, we conclude that SDSS 1624+00 is warmer and dustier than Gl 229B. Parallax measurements of SDSS 1624+00 is extremely important in determining the effective temperature.

K I 1.2432 and 1.2522 μm lines corresponding to the transition array, $4p$–$5s$ (multiplet $^2P^0$–^2S) (Wiese et al. 1966), are seen in both spectra. So it is natural to expect that the lines for the transition array, $4p$–$3d$ should be seen, because of the similar excitation and high transition probabilities. In the spectrum I, we have identified two lines at 1.1690 and 1.1773 μm corresponding to the transition array, $4p$–$3d$. In the spectrum by Strauss et al. the 1.1773 μm line is clearly detected and the 1.1690 μm is weakly detected though the signal-to-noise ratio is lower. However these lines are not apparent in the Gl 229B spectrum by Geballe et al. (1996). These lines have been detected in late M dwarfs by Kirkpatrick et al. (1993).

4. Summary

We have searched for spectral variability of SDSS 1624+00 with a 500 second time resolution over more than an hour. The suspected variation was found in water vapor absorption. Observations with a longer time baseline will be needed to confirm this variability. The integrated spectrum was compared with the previously obtained Gl 229B spectra and the model spectra. Methane absorption, the KI lines, and water vapor absorption indicate that SDSS 1624+00 is warmer and dustier than Gl 229B. Absolute flux calibration by parallax measurements of SDSS 1624+00 is needed to clarify the effective temperature problem.

We thank T. Geballe, M. Strauss, and B. Oppenheimer for providing their spectra in electronic form. We thank B. Oppenheimer, M. Iye and the referee, D. Kirkpatrick for useful comments on the manuscript. We thank the staff of the Subaru Observatory for the support of observing. This research is supported by Grants-in-Aids for Scientific Research of the Japanese Ministry of Education, Culture, Sports, and Science (No. 10640239 to TN and No. 11640227 to TT) and by the Sumitomo Foundation (TN).

References

Burgasser A. J., Kirkpatrick J. D., Brown M. E., Reid I. N., Gizis J. E., Dahn, C. C., Monet D. G., Beichman C. A. et al. 1999, ApJ 522, L65

Cuby J. G., Saracco P., Moorwood, A. F. M., D'Odorico S, Lidman C, Comeron F., Spyromilio J. 1999, A&A 347, L41

Geballe T. R., Kulkarni S. R., Woodward C. E., Sloan G. C. 1996, ApJ 467, L101

Kirkpatrick J. D., Kelley D. M., Rieke G. H., Liebert J., Allard F., Wehrse R. 1993, ApJ 402, 643

Kirkpatrick J. D., Reid, I. N., Liebert, J., Cutri, R. M., Nelson, B., Beichman, C. A., Dahn, C. C., Monet, D. G. et al. 1999, ApJ 519, 802

Leggett S. K., Toomey D. W., Geballe T. R., Brown R. H. 1999, ApJ 517, L139

Martín E. L., Basri. G., Delfosse X., Forveille T. 1997, A&A 327, L29

Nakajima T., Oppenheimer B. R., Kulkarni S. R., Golimowski D. A., Matthews, K., Durrance S. T. 1995, Nature 378, 463

Noll K. S., Geballe T. R., Marley M. S. 1997, ApJ 489, L87

Oppenheimer B. R., Kulkarni S. R., Matthews K., Nakajima T. 1995, Science 270, 1478

Oppenheimer B. R., Kulkarni S. R., Matthews K., van Kerkwijk M. H. 1998, ApJ 502, 932

Strauss M. A., Fan X., Gunn J. E., Leggett S. K., Geballe T. R., Pier, J. R., Lupton R. H., Knapp G. H. et al. 1999, ApJ 522, L61

Tinney C. G., Reid I. N. 1998, MNRAS 301, 1031

Tinney C. G., Tolley A. J. 1999, MNRAS 304, 119

Tokunaga A. T., Kobayashi N. 1999, AJ 117, 1010

Tsuji T., Ohnaka K., Aoki W. 1999, ApJ 502, L119

Wiese, W. L., Smith, M. W., Glennon, B. M., 1966, Atomic Transition Probabilities, Vol. 1. (Washington, D. C.; GPO)

Figure Captions

Figure 1. Transmission variation. The ratio of the first nearby star spectrum to the last is plotted as a function of wavelength. From the figure, it is apparent that transmission variation due to telluric water vapor was significant over the time scale of 80 minutes, and that the calibration by the simultaneously observed nearby star was essential.

Figure 2. Signal to noise ratio in a raw spectrum. A typical raw spectrum of SDSS 1624+00 in electron count (solid line) is plotted along with the square root of the sky spectrum extracted with the same aperture as the object (dotted line). The ratio of the two gives the signal-to-noise ratio obtained with a 100 second exposure.

Figure 3. Times series of combined spectra. Each spectrum corresponds to several minutes of observing. The spectra are denoted by A through H from the bottom to the eighth in the order of observing time. The top spectrum is the integrated spectrum denoted by I.

Figure 4. Spectral variability. The average spectrum of A and H in figure 3 is compared with that of E and F. The valleys of the sawtooth pattern seen in E+F is not obvious in A+H. This variation is likely due to water vapor.

Figure 5. Comparison of spectra of SDSS 1624+00 and Gl 229B. Overall Gl 229B is brighter by 1.2 mag. The Gl 229B spectrum by Geballe et al. was obtained with a higher resolution. The methane absorption longward of 1.62 μm is shallower in SDSS 1624+00 and KI lines at 1.2432 and 1.2522 μm are stronger. Finite emission is seen at the bottom of water vapor absorption between 1.34 and 1.42 μm in the SDSS 1624+00 spectrum.

Figure 6. Model spectra. D and F denote dusty and dust-free models respectively and the number indicates the effective temperature. The model spectra show some tendencies of spectral features. In the cooler model, methane and water vapor absorption are deeper and the KI lines are weaker. In the dusty model, water vapor absorption is shallower.

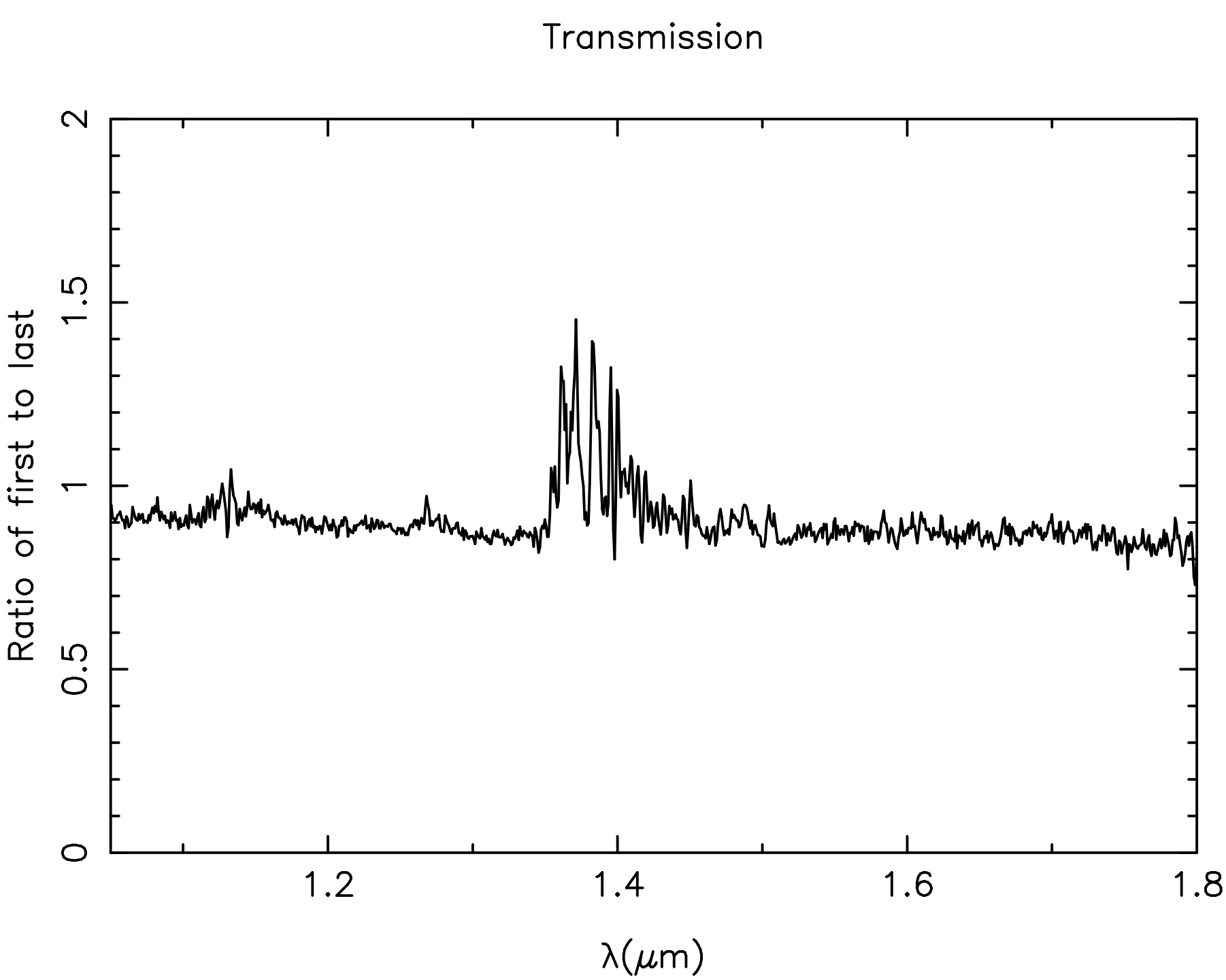
Transmission
Ratio of first to last
0
0.5
1
1.5
2
1.2
1.4
1.6
1.8
λ(μm)

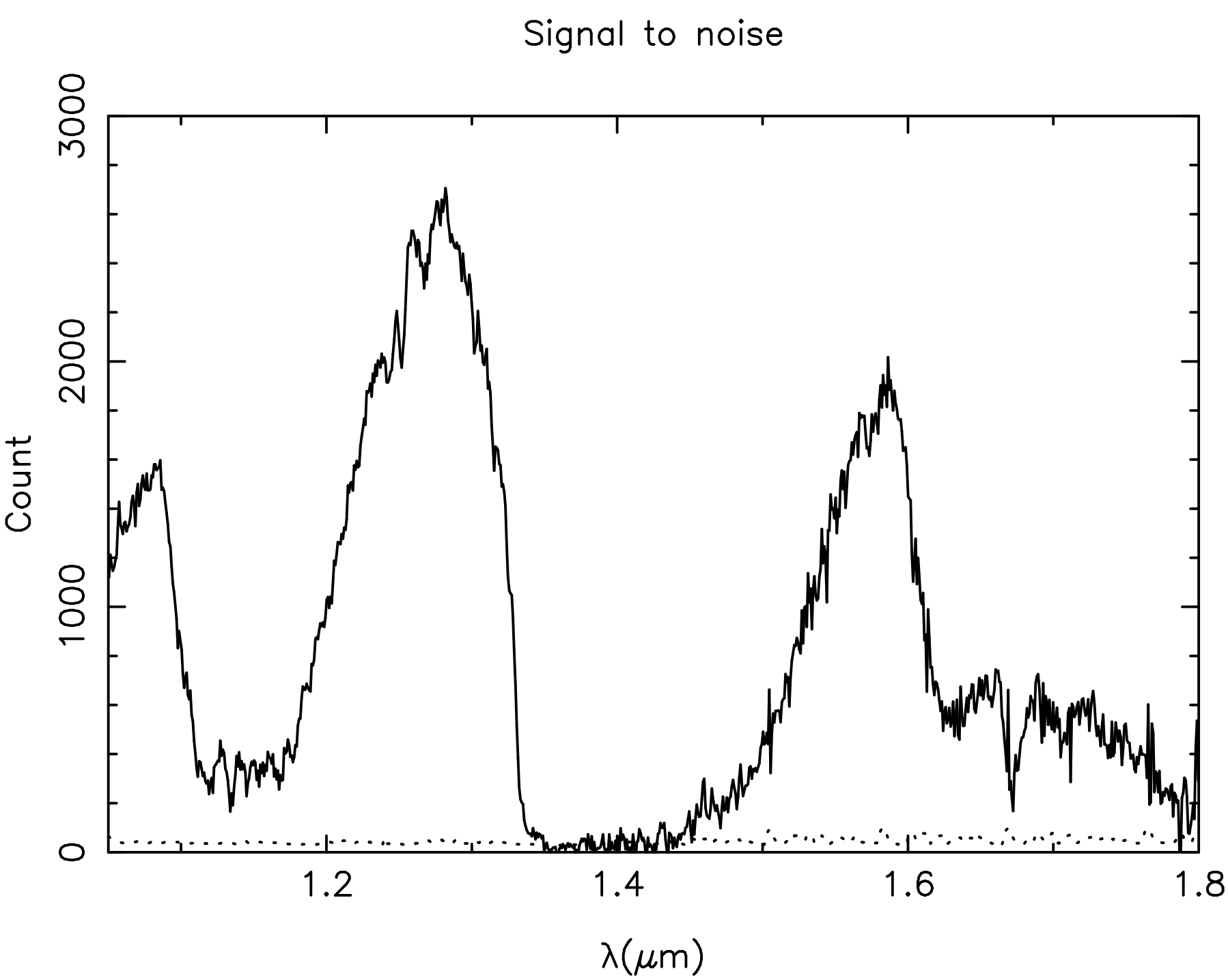
Signal to noise
Count
0
1000
2000
3000
1.2
1.4
1.6
1.8
λ(μm)

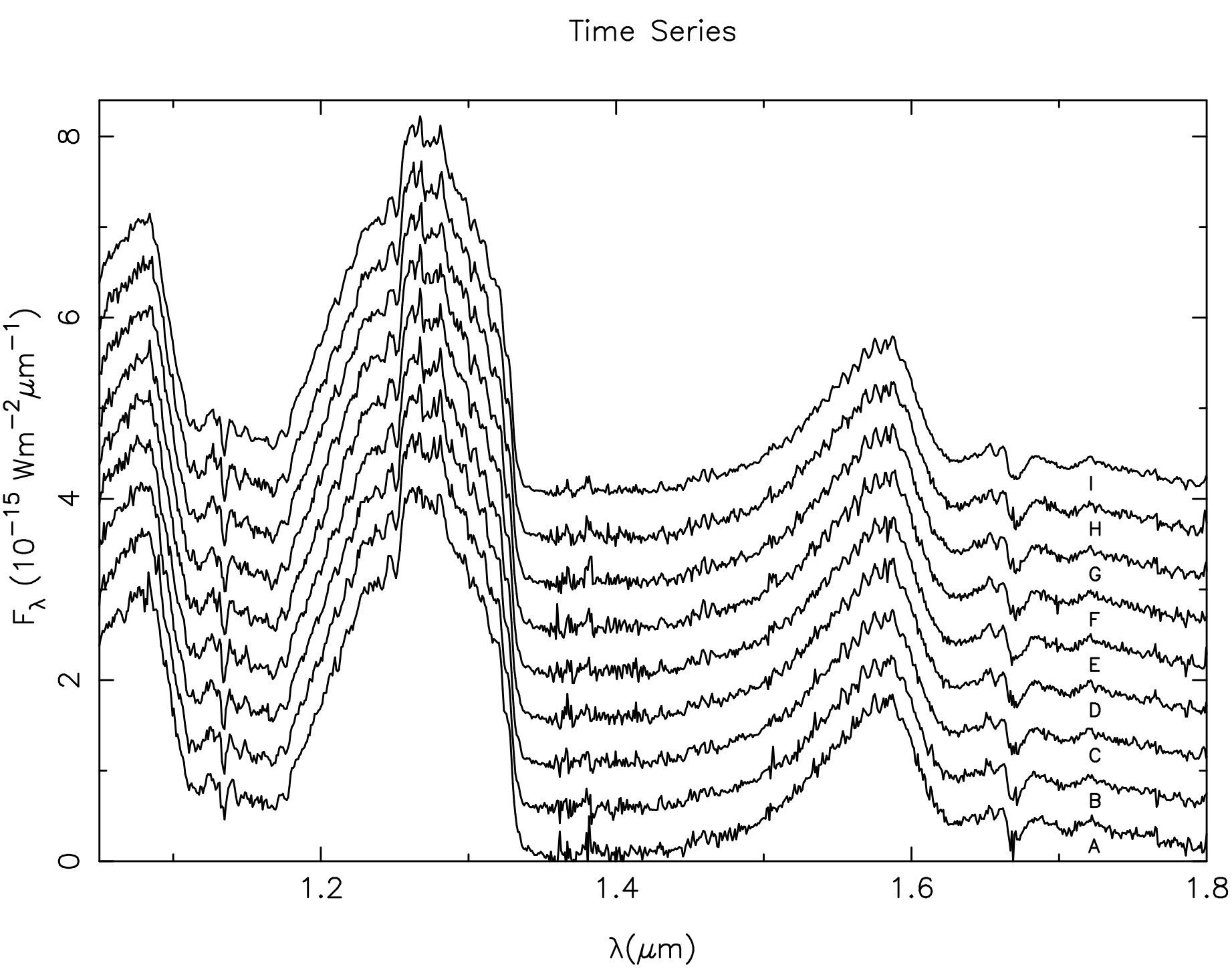
Time Series
F_λ (10^{-15} $Wm^{-2}\mu m^{-1}$)
0
2
4
6
8
1.2
1.4
1.6
1.8
λ(μm)
I
H
G
F
E
D
C
B
A

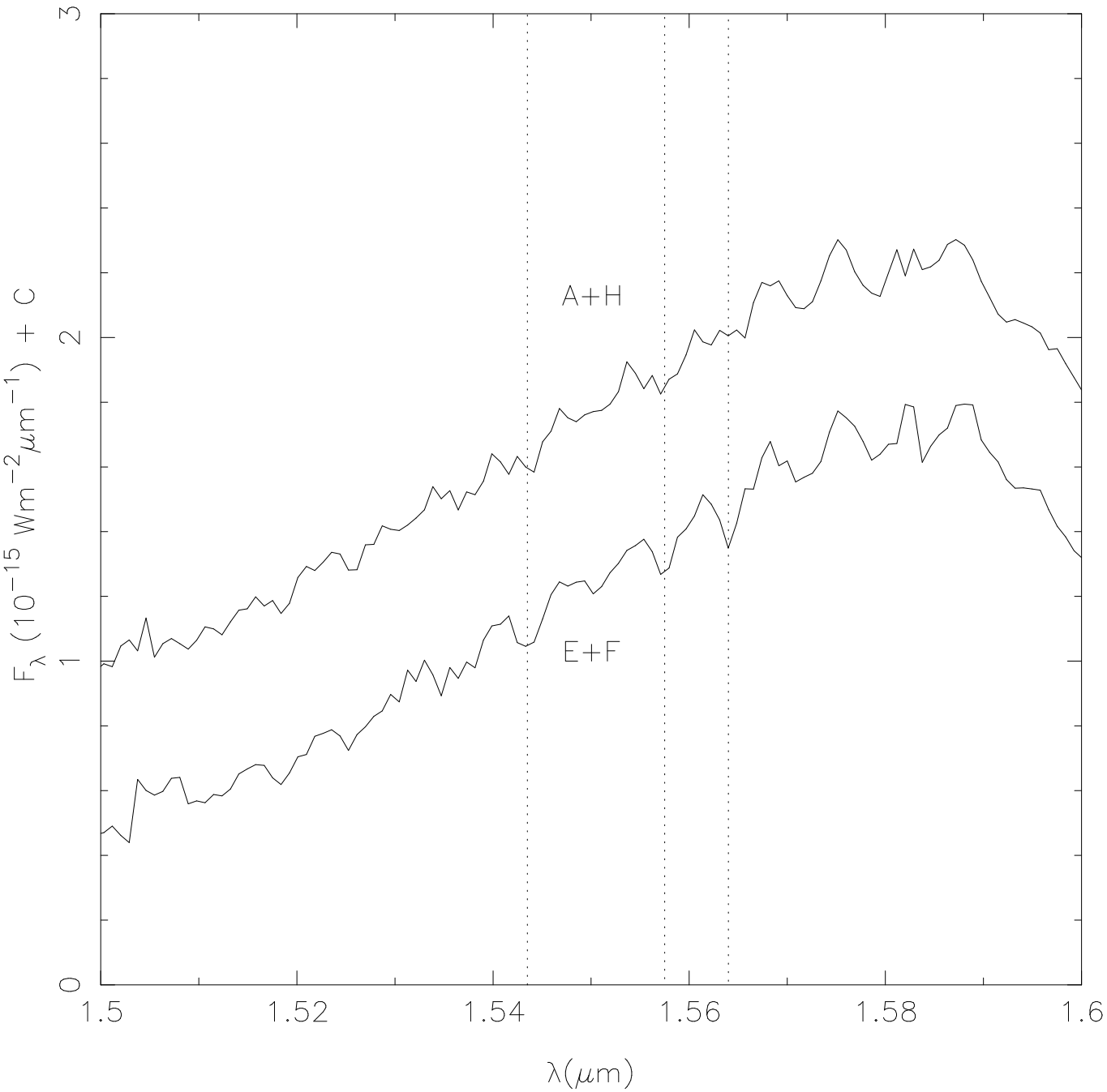
Variability
A+H
E+F
F_λ (10^{-15} $Wm^{-2}\mu m^{-1}$) + C
$\lambda(\mu m)$
0
1
2
3
1.5
1.52
1.54
1.56
1.58
1.6

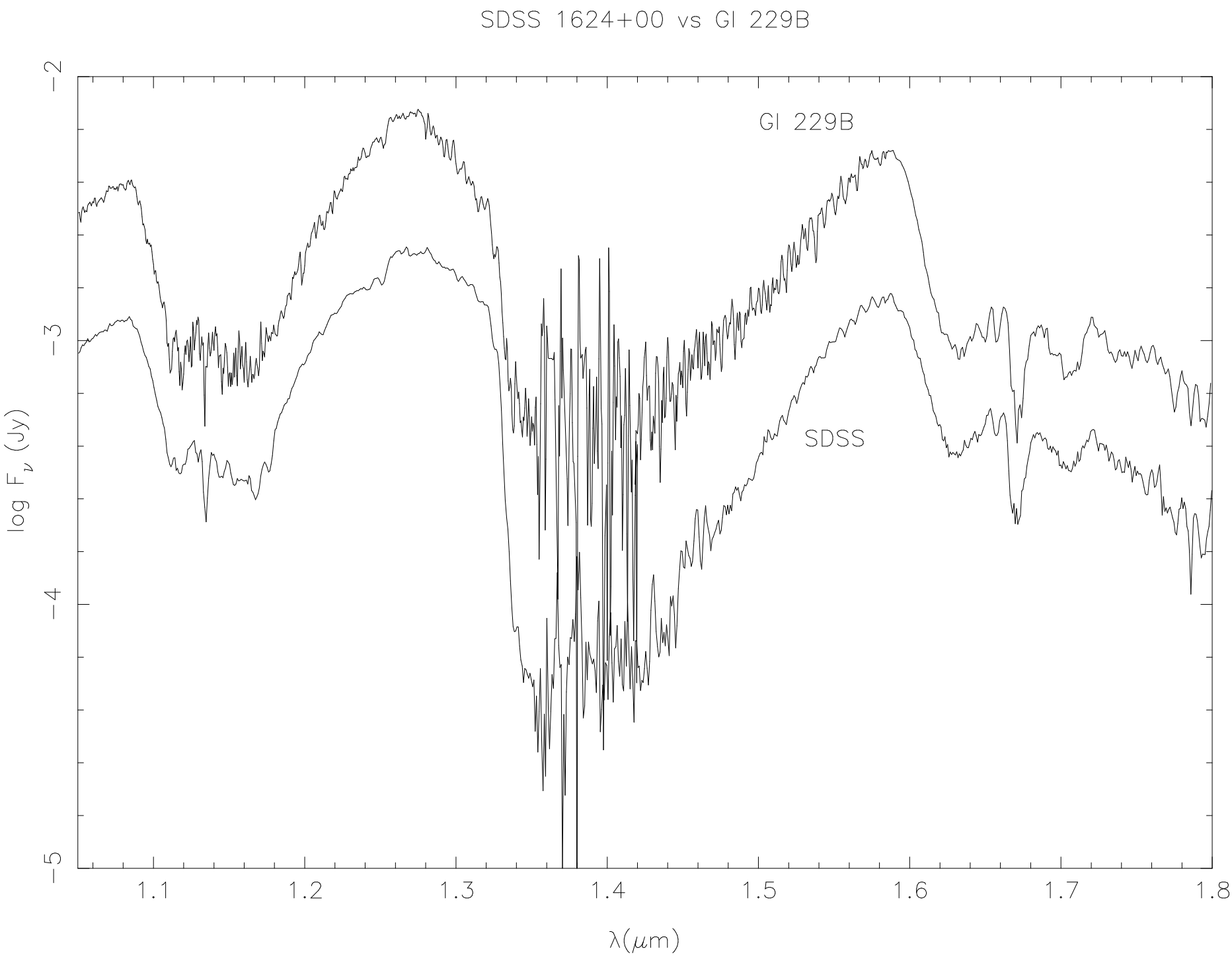
SDSS 1624+00 vs Gl 229B
Gl 229B
SDSS
log F_ν (Jy)
−2
−3
−4
−5
1.1
1.2
1.3
1.4
1.5
1.6
1.7
1.8
λ(μm)

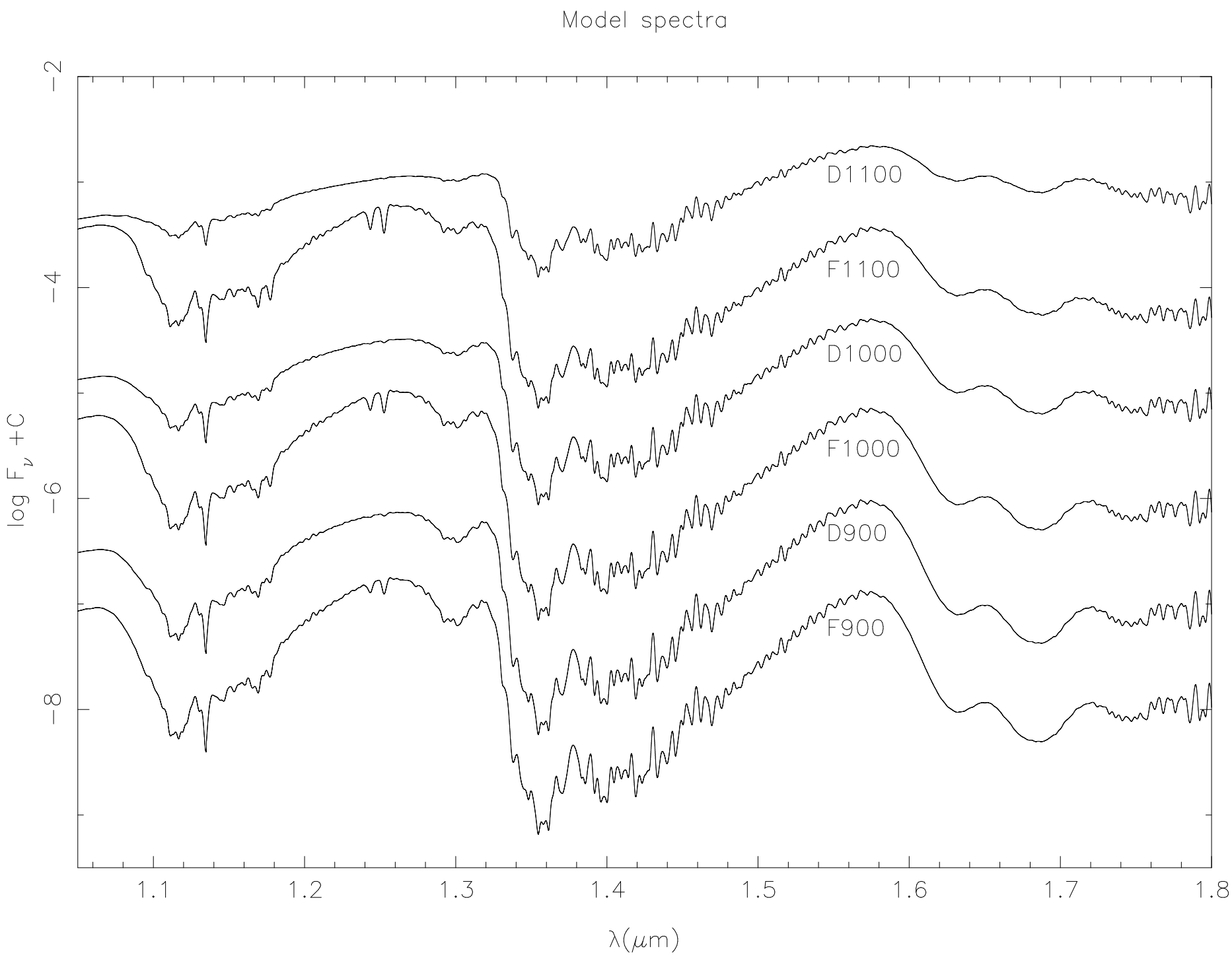
Model spectra
D1100
F1100
D1000
F1000
D900
F900
log F_ν +C
−2
−4
−6
−8
1.1
1.2
1.3
1.4
1.5
1.6
1.7
1.8
λ(μm)